ROYAL SOCIETY OPEN SCIENCE

rsos.royalsocietypublishing.org

Research

Cite this article: Llanos J, Brito I, Espinoza D, Sekar R, Manidurai P. 2018 A down-shifting Eu^{3+}-doped Y_2WO_6/TiO_2 photoelectrode for improved light harvesting in dye-sensitized solar cells. *R. Soc. open sci.* **5**: 171054. http://dx.doi.org/10.1098/rsos.171054

Received: 3 August 2017
Accepted: 8 January 2018

Subject Category:
Chemistry

Subject Areas:
materials science

Keywords:
dye-sensitized solar cells, down-shifting, photoelectrode, lanthanide ion

Author for correspondence:
J. Llanos
e-mail: jllanos@ucn.cl

This article has been edited by the Royal Society of Chemistry, including the commissioning, peer review process and editorial aspects up to the point of acceptance.

THE ROYAL SOCIETY PUBLISHING

A down-shifting Eu^{3+}-doped Y_2WO_6/TiO_2 photoelectrode for improved light harvesting in dye-sensitized solar cells

J. Llanos[1], I. Brito[2], D. Espinoza[3], Ramkumar Sekar[4] and P. Manidurai[4]

[1]Department of Chemistry, Universidad Católica del Norte, Avda. Angamos 0610, Antofagasta, Chile
[2]Department of Chemistry, Universidad de Antofagasta, Avda. Angamos 0601, Antofagasta, Chile
[3]Department of Chemistry, Universidad de Chile, Las Palmeras 3425, Santiago, Chile
[4]Department of Physics, Universidad de Concepcion, Barrio Universitario, Casilla 160-C, Concepción, Chile

JL, 0000-0002-0804-3166

$Y_{1.86}Eu_{0.14}WO_6$ phosphors were prepared using a solid-state reaction method. Their optical properties were analysed, and they was mixed with TiO_2, sintered, and used as a photoelectrode (PE) in dye-sensitized solar cells (DSSCs). The as-prepared photoelectrode was characterized by photoluminescence spectroscopy, diffuse reflectance, electrochemical impedance spectroscopy (EIS) and X-ray diffraction. The photoelectric conversion efficiency of the DSSC with TiO_2:$Y_{1.86}Eu_{0.14}WO_6$ (100:2.5) was 25.8% higher than that of a DSCC using pure TiO_2 as PE. This high efficiency is due to the ability of the luminescent material to convert ultraviolet radiation from the sun to visible radiation, thus improving the solar light harvesting of the DSSC.

1. Introduction

Dye-sensitized solar cells (DSSCs) are part of this third generation, and they have attracted considerable attention because of their low cost, easy fabrication and relatively high conversion efficiencies [1,2]. DSSCs were proposed by O'Regan and Grätzel in 1991 [3]. However, the poor response of DSSCs to red and near-infrared (NIR) light has been a significant impediment

for achieving higher photocurrents and efficiencies. Therefore, to develop competitive DSSC technology, further increasing their efficiency by widening their operational spectral range is necessary.

The spectral response of conventional DSSCs is very narrow compared to the whole wavelength range of sunlight. The band between 400 and 700 nm only accounts for approximately 43% of the sun's total radiant energy [4]. To harvest energy in the red and NIR regions of the solar spectrum, new types of dyes, quantum dots and co-sensitizers are currently under development [5–8]. All of these routes still suffer from some disadvantages, however, such as: (i) the new dyes do not absorb at wavelengths above 750 nm, i.e. in the red region; (ii) organic dyes decompose relatively easily upon interacting with the I_3^- electrolyte; and (iii) quantum dots are sensitive to the presence of moisture or oxygen and have restrictions for their use in sensitized solar cells [9,10]. A novel way to enhance the conversion efficiency in DSSCs is the use of down-shifting (DS), down-conversion (DC) and up-conversion (UC) luminescent materials as components of the solar cells. Generally, DS, DC and UC materials consist of rare earth (RE)-doped inorganic host materials. The intra-*4f* transitions in RE-doped luminescent materials can be efficiently used as either NIR-to-visible up-convertors or ultraviolet (UV)-to-visible down-convertors for applications in DSSCs.

On the other hand, the literature reports that exposure to UV light produces serious damage to the DSSC since the iodine present in the electrolyte is irreversibility consume under UV light [11]. Down-conversion or down-shifting phosphors are suitable materials for reducing this disadvantage in dye-sensitized solar cells. Recently, Zhang *et al*. described how the use of the inorganic phosphors LAVO4:Dy3+ introduced into a DSSC, not only improves the electrical conversion efficiency (*ca* 23%), but also expands considerably the lifetime of the solar cell [12].

This paper is part of our continuing research on the synthesis, applications, characterization and luminescent properties of inorganic phosphors containing rare-earth cations [13–16]. In this report, we focused on the preparation of Eu^{3+}-doped Y_2W0_6 and its application in photoelectrodes (PE) in DSSCs in order to investigate the possibility of increasing the spectral response of DSSCS using down-shifting luminescent materials.

2. Experimental

2.1. Materials

All chemical reagents including Eu_2O_3, Y_2O_3, WO_3, TiO_2 nanopowder (21 nm), I_2, LiI, tetrabutylammonium iodide, and t-octylphenoxypolyethoxyethanol as emulsification agent (Triton X-100) were analytical grade and supplied by Sigma-Aldrich. Conducting glass plates of indium tin oxide (ITO) with a surface resistivity of 8–12 $\Omega\,sq^{-1}$ and the sensitizing dye N-719 ($RuL_2(NCS)_2$:2TBA (L = 2,2′-bipyridyl-4,4′-dicarboxylic acid)) were also purchased from Sigma-Aldrich and used without further treatment.

2.2. Preparation of Eu^{3+}-doped Y_2W0_6 nanoparticles

The Y_2WO_6:Eu^{3+} phase was prepared via a solid-state reaction at high temperature [17,18]. All phosphors were synthesized from a thoroughly ground mixture of the corresponding oxides, Y_2O_3, Eu_2O_3 and WO_3, in stoichiometric proportions. The mixtures were placed in an alumina boat and heated to 973 K for 10 h before cooling below 400 K. The sample was removed from the crucible, ground into a powder, and reheated for 10 h at 1273 K. This procedure was repeated, and the sample was finally heated to 1373 K for another 10 h. All of these synthetic processes were performed under an air atmosphere. Optical inspection of the products showed homogeneous white powders.

Powder X-ray diffraction (PXRD) data were collected using a Bruker D8 Advance diffractometer fitted with a graphite monochromator using Cu Kα radiation ($\lambda = 1.54057$ Å) across the range of $10° \leq 2\theta \leq 60°$ to determine the phase purity. The experimental PXRD patterns for the doped and un-doped samples were almost in perfect agreement with those reported in the inorganic crystal structure database (ICSD) database [19].

2.3. Preparation of dye-sensitized solar cell

Different amounts of $Y_{1.86}Eu_{0.14}WO_6$ (1%, 2%, 2.5% and 3%) were dispersed in a TiO_2 sol, ultrasonicated, stirred for about 30 min and finally used as slurry. The PE was prepared by the doctor-blade technique [20,21]. After air-drying, the electrodes were sintered at 450°C for 30 min and soaked in an N-719

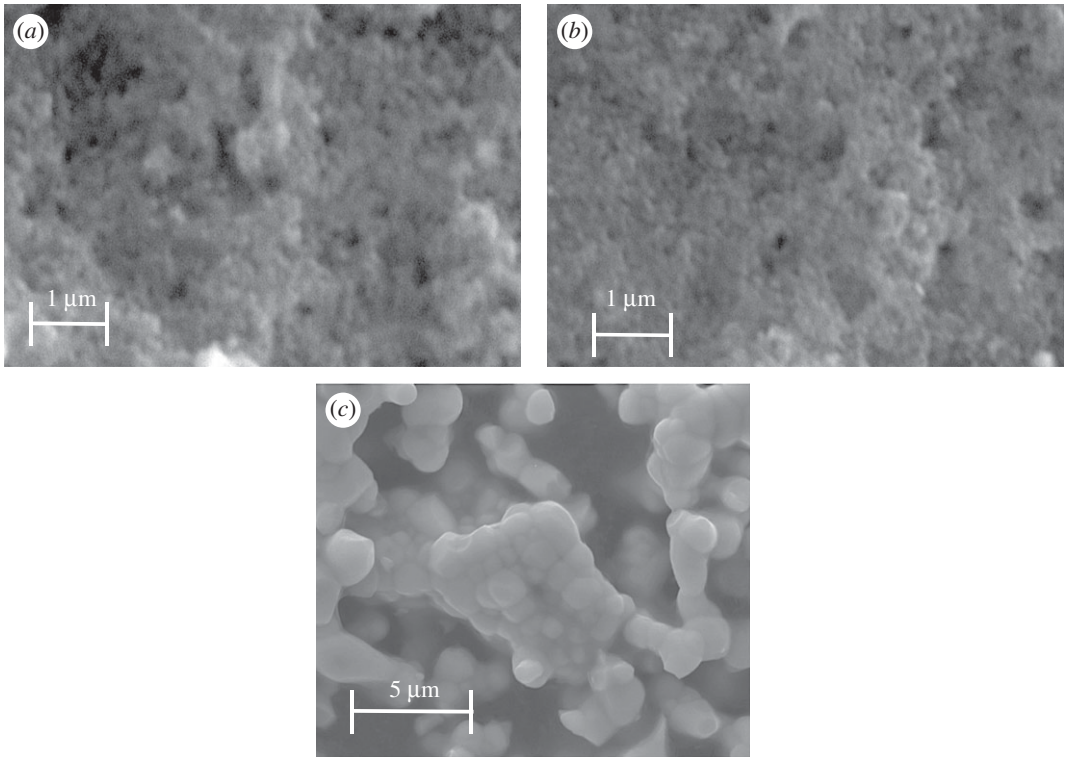

Figure 1. SEM images of (*a*) TiO_2, (*b*) $TiO_2/Y_{1.86}Eu_{0.14}WO_6$ (100:2.5) and (*c*) $Y_{1.86}Eu_{0.14}WO_6$.

dye solution (3×10^{-4} M in ethanol) for 24 h. For comparison, a PE without $Y_{1.86}Eu_{0.14}WO_6$ (i.e. pure TiO_2) was also prepared. Finally, the DSSC was assembled by filling an electrolyte solution (0.60 M tetrabutylammonium iodide, 0.05 M I_2, and 0.10 M LiI in acetonitrile) between the dye-sensitized $Y_{1.86}Eu_{0.14}WO_6/TiO_2$ electrode and a platinized conducting glass electrode. Both electrodes were clipped together, and a cyanoacrylate adhesive was used as a sealant to prevent the electrolyte solution from leaking. For comparison, a DSSC was prepared with the pure TiO_2 PE using the same method.

2.4. Characterization

The phase purities were determined via PXRD analysis (vide supra). The nanocrystalline $Y_{1.86}Eu_{0.14}WO_6$ phosphor surface morphologies were determined via scanning electron microscopy (SEM, JEOL, JSM-6360LV). The photoluminescence (PL) spectra were measured using a JASCO FP-6500 spectrofluorometer. All of the spectra were collected at room temperature. The sample quantities were identical across all experiments so that the photoluminescence intensities could be compared. A Perkin-Elmer Lambda 20 UV-Vis spectrophotometer equipped with a Labsphere RSA-PE-20 diffuse reflectance accessory was used to measure the diffuse reflectance of the samples over the range of 200–600 nm (6.2–2.1 eV). The photovoltaic test of the DSSCs was performed using a PET cell tester (model CT80AAA, Photo Emission Tech., Inc. USA), under simulated AM 1.5 solar illumination of one sun (100 mW cm^{-2}) from a 300 W Xe lamp. The intensity was adjusted using a calibrated c-Si solar cell. The I–V measurements were attained using a Keithley Sourcemeter model 2400. The electrochemical impedance spectroscopy (EIS) analysis were carried out with Solartron 1280 impedance analyser. Nyquist plots were measured at open circuit voltage (V_{oc}) over a frequency range of 1–10^4 under one-sun illumination. To determine the amount of dye desorbed from the photoelectrode a 1 M solution of NaOH was used and the UV-Vis spectra were recorded in a Perkin-Elmer Lambda 25 spectrophotometer.

3. Results and discussion

The crystallite morphology of $Y_{1.86}Eu_{0.14}WO_6$ was inspected via SEM. The results revealed that the samples are spherical and exhibit some tendency to aggregate, as shown in figure 1 [18]. The morphology of the layers was also inspected by SEM. Figure 1 shows the typical SEM images of bare TiO_2 and the

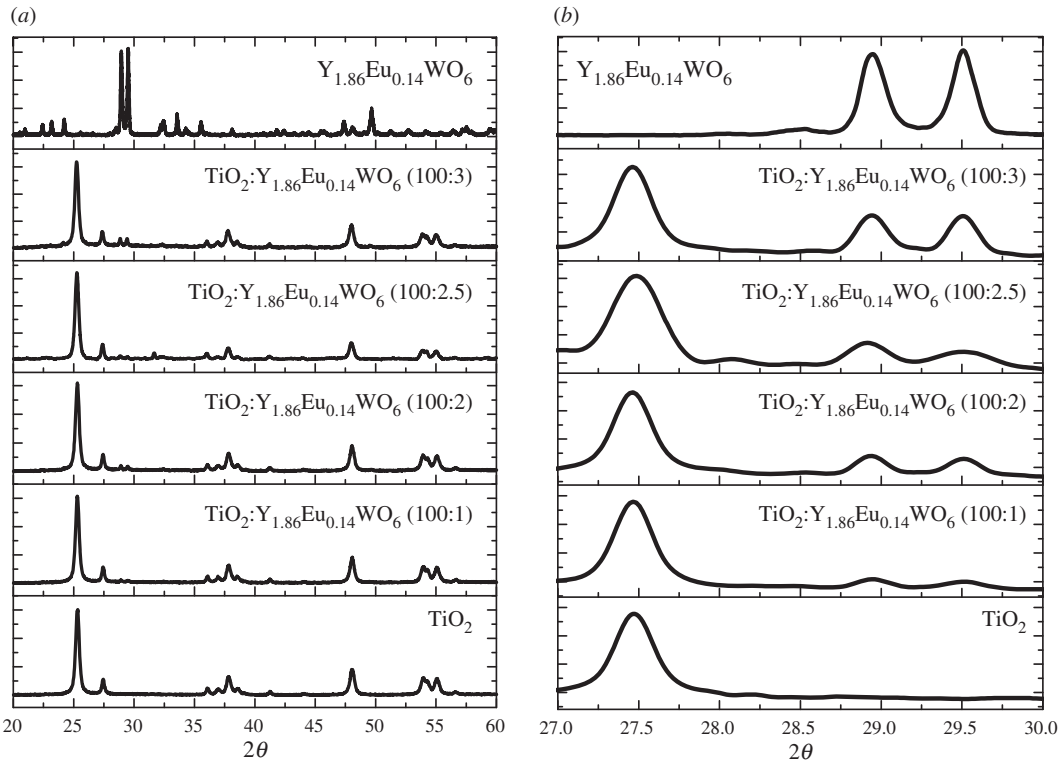

Figure 2. (*a*) XRD patterns of TiO_2 mixed with different content of $Y_{1.86}Eu_{0.14}WO_6$. (*b*) XRD patterns in the 2θ region of 27–30°.

doped samples. No remarkable differences were observed. The phosphor was embedded within the structure of TiO_2, which is an important characteristic to obtain a good dye distribution [22].

Additionally, the Scherrer equation ($D = 0.90\lambda/\beta\cos\theta$) can estimate the crystallite size of the luminescent material from the PXRD results if the crystals are smaller than 1000 Å. In this equation, D is the average grain size, λ is the wavelength of the radiation used in the diffraction experiments (vide supra), θ is the diffraction angle and β is the full width at half maximum (FWHM) of the observed peak [23,24]. Since small angular differences are associated with large spatial distances (inverse space), the broadening of a diffraction peak is expected to reflect some scaling feature in the crystal. The strongest diffraction peak located at $2\theta = 29.5°$ was used to calculate the grain size of $Y_{1.86}Eu_{0.14}WO_6$. Our results indicate that the crystallite size for the sample is approximately 62 nm. The PXRD patterns of pure TiO_2 and $Y_{1.86}Eu_{0.14}WO_6$ (1%, 2%, 2.5% and 3% by weight) dispersed in TiO_2 and pure $Y_{1.86}Eu_{0.14}WO_6$ are displayed in figure 2.

The corresponding UV-Vis diffuse reflectance spectra of the pure TiO_2 and the corresponding $Y_{1.86}Eu_{0.14}WO_6$ (1%, 2%, 2.5% and 3% in weight) dispersed in TiO_2 are superimposed in the figure 3. The band edges are analogous and indicate a band gap energy between 3.13 and 3.15 eV. The commonly reported value for the energy band gap of TiO_2 is 3.2 eV [25]. Ground state diffuse reflectance absorption studies for the as-prepared photoelectrodes show that semiconductor properties of the TiO_2 were not obstructed by the inorganic phosphor.

The synthesized phosphor shows the typical excitation and emission bands. The photoluminescence excitation spectrum (PLE) exhibits a broad charge transfer band centred at about 300 nm along with very weak f-f transitions at about 395 nm ($^7F_0 \rightarrow {}^5L_6$), 465 nm ($^7F_0 \rightarrow {}^5D_2$) and 540 nm ($^7F_0 \rightarrow {}^5D_1$). The broad, intense band consists of overlapping O^{2-}-Eu^{3+} and O^{2-}-W^{6+} charge transfer bands. Upon excitation at 300 nm, the resulting emission spectrum originates from the transition between the $^5D_0$ excited state to the ^7F_j ground states ($j = 0, 1, 2, 3, 4$) for the $4f^6$ configuration of Eu^{3+}, with the most prominent electric dipole transition, $^7D_0 \rightarrow {}^5F_2$, centred at about 610 nm. Figure 4 shows the excitation and emission spectra of $Y_{1.86}Eu_{0.14}WO_6$ compared with the absorbance of N-719 dye.

Using ITO conductive glass as a substrate, the TiO_2:$Y_{1.86}Eu_{0.14}WO_6$ photoelectrodes were prepared using the doctor-blade technique [20,21]. The emission spectra of the film electrodes at a wavelength of 300 nm exhibit an intense peak at 610 nm. The effect of the phosphor phase on the emission intensity is shown in figure 5. The emission intensity reaches a maximum with the TiO_2:$Y_{1.86}Eu_{0.14}WO_6$ (100:2.5)

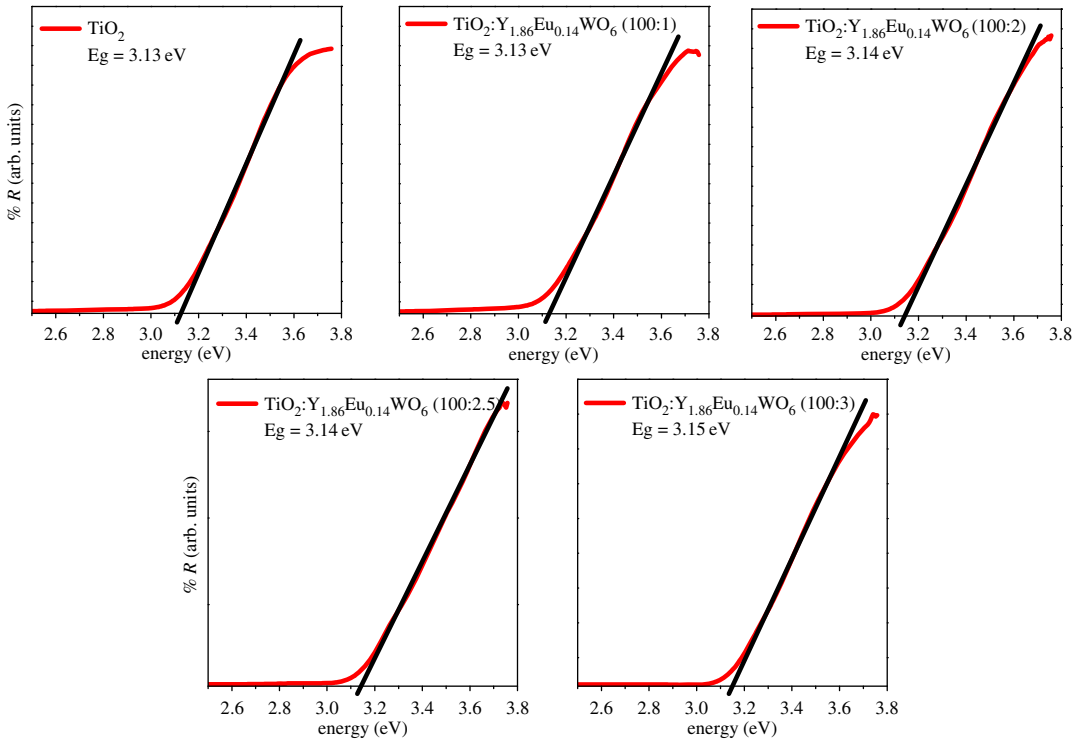

Figure 3. UV-visible diffuse reflectance curves of TiO_2 mixed with different content of $Y_{1.86}Eu_{0.14}WO_6$. The band gaps of pristine TiO_2 and TiO_2 with different contents of phosphors were calculated by the Tauc's plot method.

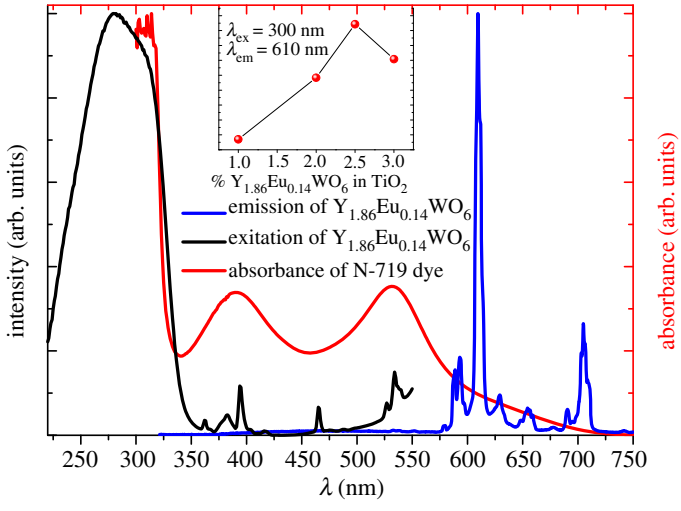

Figure 4. Excitation and emission spectra of $Y_{1.86}Eu_{0.14}WO_6$ compared with the absorbance of N-719 dye.

electrode (see inset figure 4). The luminescent material can convert the UV radiation from the sun to visible radiation, thus improving the solar light harvesting of the DSSC.

Figure 6 shows the photovoltaic performance of DSSC using the mixed TiO_2:$Y_{1.86}Eu_{0.14}WO_6$ (100:2.5) and pure TiO_2 PEs. To obtain significant data, five DSSCs were prepared with and without 2.5 wt% of the luminescent material. When the PE consists of pure TiO_2, the DSSC has a short-circuit current density (J_{sc}) of 8.6 mA cm^{-2}, an open circuit voltage (V_{oc}) of 0.76 V, a field-factor (FF) of 0.48 and a photoelectric conversion efficiency (PCE) of 3.1%. The DSSCs with TiO_2:$Y_{1.86}Eu_{0.14}WO_6$ (100:2.5) photoelectrode show a J_{sc} of 12.3 mA cm^{-2}, a V_{oc} of 0.76 V, a FF of 0.43 and a PCE of 3.9%. The DSSC with the down-shifting material exhibits a higher J_{sc} due to the increase in photo-generated photons in the visible region converted from the UV region of the solar spectrum. By the other hand, the Rs and Rsh values for the DSSC using the mixed TiO_2:$Y_{1.86}Eu_{0.14}WO_6$ (100:2.5) photoelectrode were 9.8 Ω and 1657 Ω, respectively. Whereas for the DSSC using bare TiO_2 the values were and 10.8 Ω cm^2 and 2036 Ω cm^2, respectively.

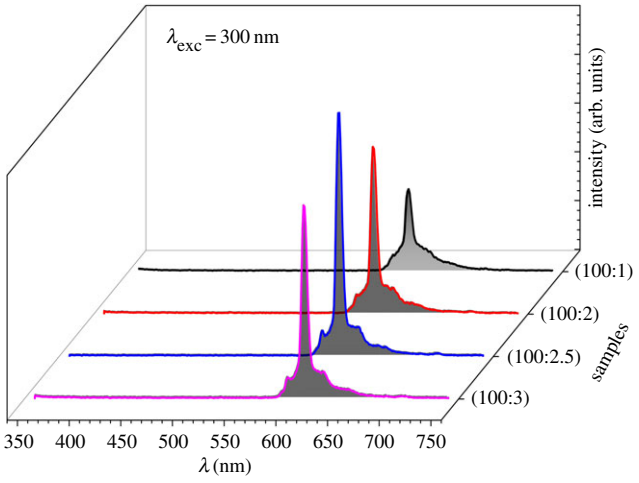

Figure 5. Emission spectra of the film electrodes at wavelength of 300 nm.

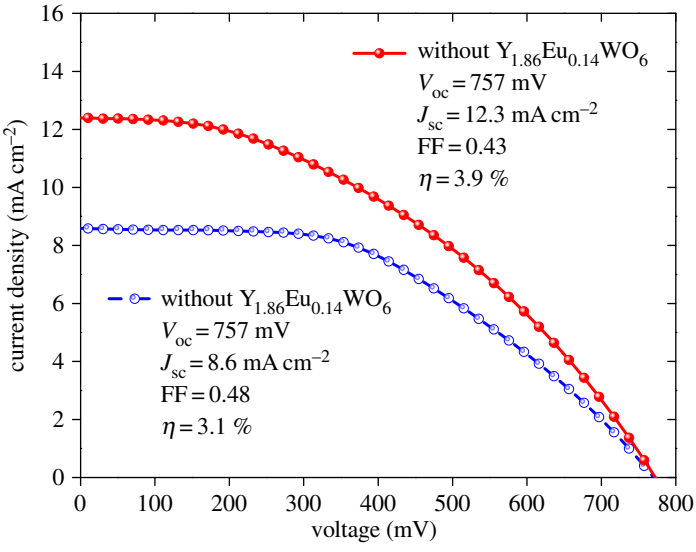

Figure 6. Current density–voltage characteristics for bare and phosphor doped TiO_2 based DSSCs under illumination of simulated solar light (AM 1.5, 100 mW cm^{-2}).

Table 1. Photovoltaic (PV) properties of bare and phosphor doped TiO_2 based DSSCs.

DSSC	J_{sc} (mA cm^{-2})	V_{oc} (mV)	FF	PCE (%)	dye (mol cm^{-2})
TiO_2	8.6	757	0.48	3.1	4.61×10^{-9}
TiO_2:$Y_{1.86}Eu_{0.14}WO_6$	12.3	757	0.43	3.9	2.94×10^{-9}

To determine the amount of dye loading in both photoanodes (TiO_2 and TiO_2:$Y_{1.86}Eu_{0.14}WO_6$), the photoelectrodes were soaked in a 1 M NAOH solution for 12 h. The absorption spectra of the desorbed dye represented the amount of dye absorbed for the photoanodes. Figure 7 shows the UV-Vis absorbance spectra of the dye molecules detached from both photoelectrodes. The amount of absorbed N-719 was 4.61×10^{-9} and 2.94×10^{-9} mol cm^{-2} for TiO_2 and TiO_2:$Y_{1.86}Eu_{0.14}WO_6$, respectively. Remarkable is the fact that the TiO_2:$Y_{1.86}Eu_{0.14}WO_6$ (100:2.5) show less absorption than the pristine TiO_2, their photovoltaic properties are better. The DSSC parameters obtained in our study are shown in table 1.

The incident photon-to-current efficiency (IPCE) for the dye-sensitized solar cell of DSSC with down-shifting material and with pure TiO_2 were measured and are shown in figure 8. The IPCE of the

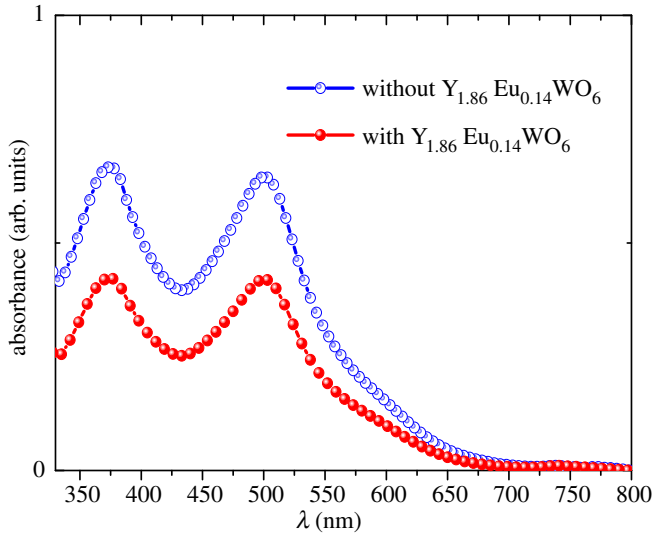

Figure 7. UV-Vis absorbance spectra of the N-719 molecules detached from the photoanodes.

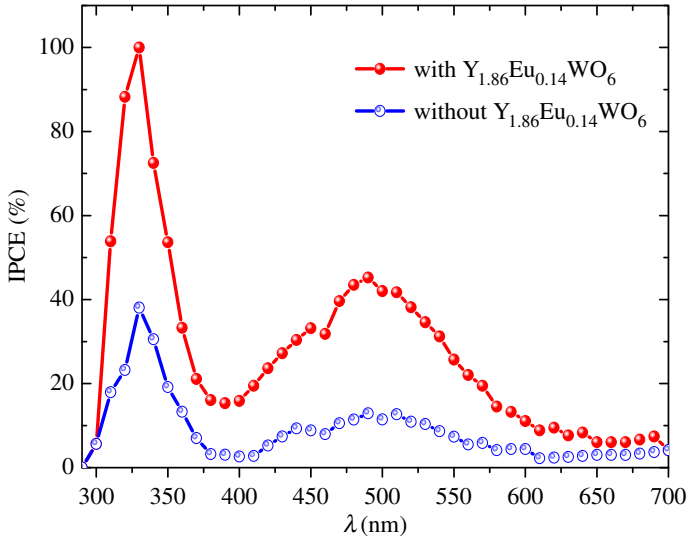

Figure 8. Incident photon to current conversion efficiency (ICPE) curves for bare and phosphor doped TiO_2 based DSSCs.

dye-sensitized solar cell depends on the incident light harvesting and light scattering [26,27]. The enhancement of the IPCE in the range 300–400 nm can be associated with $^5D_0 \rightarrow {}^7F_1$, $^5D_0 \rightarrow {}^7F_2$ and $^5D_0 \rightarrow {}^7F_4$ transitions of Eu^{3+} under excitation at 300 nm (CTB O^{2-}-Eu^{3+}). The higher IPCE is attributed to the down-shifting from the ultraviolet light to visible light due to the presence of $Y_{1.86}Eu_{0.14}WO_6$ in the photoelectrode [28]. The ultraviolet light converted to visible was reabsorbed by the N-719 dye causing higher IPCE [29]. Our results are in agreement with those reported in the literature where the DS or DC phosphor layers were directly integrated into the DSSC surface to increase the spectral response of the cell [30].

On the other hand, the electrochemical impedance spectroscopy (EIS) is an important tool to understand the transport properties within an electrochemical system [31–34]. The EIS spectra of the DSSCs with different photoelectrodes were analysed over a frequency range of 1–10 kHz under one-sun illumination at V_{oc}. The recorded spectra show a circle at low frequency corresponds to the impedance of TiO_2/electrolyte interface. Figure 9 shows Nyquist plots of DSSC made with and without luminescent material under one-sun illumination. As shown in figure 9, the smallest circle corresponds to phosphor doped DSSC, which means a decrease in the interfacial resistance and an increase in the efficiency of the cell. This also indicates that the charge transport resistance is lower for the DSSC

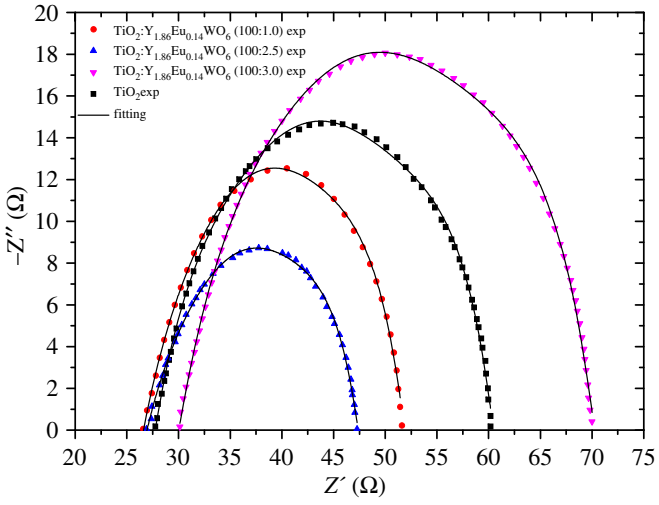

Figure 9. Nyquist plots of the DSSCs based on $TiO_2/Y_{1.86}Eu_{0.14}WO_6$ (100:0; 100:1; 100:2.5 and 100:3) photoelectrodes measured at V_{oc} under one-sun illumination.

using the mixed TiO_2:$Y_{1.86}Eu_{0.14}WO_6$ (100:2.5) (3.6 Ω) than that using the bare TiO_2 (4.8 Ω). This also indicates less impedance suggesting a faster electron transport, and consequently an improvement in the conversion efficiency. If the concentration of DS phosphor exceeds 2.5%, the charge carrier transportation is hindered. According to Yin *et al.*, the TiO_2:$Y_{1.86}Eu_{0.14}WO_6$ (100:2.5) must have the smaller Rct value. This implies that the electron transfer from the TiO_2:$Y_{1.86}Eu_{0.14}WO_6$ to the electrolyte is more efficient than that of the pristine TiO_2 electrode [35].

More work in order to prepare $Y_{2-x}Eu_xWO_6/TiO_2$ core-shell nanoparticles as photoelectrode (PE) for use in dye sensitized solar cells (DSSCs) is in progress.

4. Conclusion

The optimized TiO_2:$Y_{1.86}Eu_{0.14}WO_6$ (100:2.5) mixture was used as a photoelectrode to fabricate DSSCs that were more efficient than DSSCs based on pure TiO_2 photoactive electrodes. The solar conversion efficiency for a DSSC with the mixed PE reached 3.9%, which is 25.8% higher than that of a DSCC using pure TiO_2 as the PE.

On the other hand, ground state diffuse reflectance absorption measurements indicated that the addition of the down-shifting phosphor does not affect the semiconductor character of TiO_2. Finally, in this work we demonstrated that the down-shifted luminescence could be an effective way to improve the sunlight harvesting of solar cells. The last result is supported by electrochemical impedance spectroscopy and optical measurements.

Data accessibility. General method, materials used and data sheets figures of this article are available at Dryad (http://dx.doi.org/10.5061/dryad.t04k1) [36].

Authors' contributions. J.L. designed the study and wrote the manuscript; D.E. and R.S. performed the experiments; I.B. and P.M. analysed the results and revised the manuscript. All authors gave final approval for publication

Competing interests. The authors declare no competing interest.

Funding. This work was financially supported by the Comision Nacional de Investigacion Cientifica y Tecnologica of Chile (CONICYT) Grant 1130248 (FONDECYT), Postdoctoral program (no. 3150213), Grant 1130802 (FONDECYT).

Acknowledgements. Authors thank Laboratorio de Servicios Analíticos (Universidad Católica del Norte) for providing the facilities to use the UV-Vis spectrophotometer.

References

1. Ye M, Wen X, Wang M, Iocozzia J, Zhang N, Lin C, Lin Z. 2015 Recent advances in dye-sensitized solar cells: from photoanodes, sensitizers and electrolytes to counter electrodes. *Mater. Today* **18**, 155–162. (doi:10.1016/j.mattod.2014.09.001)
2. Shalini S, Balasundaraprabhu R, Satish Kumar T, Prabavathy N, Senthilarasu S, Prasanna S. 2016 Status and outlook of sensitizers/dyes used in dye sensitized solar cells (DSSC): a review. *Int. J. Energy Res.* **40**, 1303–1320. (doi:10.1002/er.3538)
3. O'Regan B, Grätzel M. 1991 A low-cost, high-efficiency solar cell based on dye-sensitized. *Nature* **353**, 737–740. (doi:10.1038/353737a0)
4. Gao X-D, Li X-M, Gan X-Y. 2013 Enhancing the light harvesting capacity of the photoanode films. In

Dye-sensitized solar cells in solar cells: research and application perspectives. (ed. A Morales-Acevedo), pp. 169–202. Rijeka, Croatia: InTech. (doi:10.5772/51633)

5. Chen BS, Chen DY, Chen CL, Hsu CW, Hsu HC, Wu KL, Liu SH, Chou PT, Chi Y. 2011 Donor-acceptor dyes with fluorine substituted phenylene spacer for dye-sensitized solar cells. *J. Mater. Chem.* **21**, 1937–1945. (doi:10.1039/c0jm02433c)
6. Soliman AA, Amin MA, El-Sherif AA, Sahin C, Varlikli C. 2017 Synthesis, characterization and molecular modeling of new ruthenium(II) complexes with nitrogen and nitrogen/oxygen donor ligands. *Arabian J. Chem.* **10**, 389–397. (doi:10.1016/j.arabjc.2015.04.001)
7. Hardin BE *et al.* 2009 Increased light harvesting in dye-sensitized solar cells with energy relay dyes. *Nat. Photonics.* **3**, 406–411. (doi:10.1038/NPHOTON.2009.96)
8. Hu F, Xia Y, Guan Z, Yin X, He T. 2012 Low temperature fabrication of ZnO compact layer for high performance plastic dye sensitized ZnO solar cell. *Electrochim. Acta* **69**, 97–101. (doi:10.1016/j.electacta.2012.02.084)
9. Jun HK, Careem MA, Arof AK. 2013 Quantum dot-sensitized solar cells—perspective and recent developments: a review of Cd chalcogenide quantum dots as sensitizers. *Renew. Sust. Energy Rev.* **22**, 148–167. (doi:10.1016/j.rser.2013.01.030)
10. Kuang D, Walter P, Nuesch F, Kim S, Ko J, Comte P, Zakeeruddin SM, Nazeeruddin MK, Gratzel M. 2007 Co-sensitization of organic dyes for efficient ionic liquid electrolyte-based dye-sensitized solar cells. *Langmuir* **23**, 10 906–10 909. (doi:10.1021/la702411n)
11. Kato N, Takeda Y, Higuchi K, Takeichi A, Sudo E, Tanaka H, Motohiro T, Sano T, Toyoda T. 2009 Degradation analysis of dye-sensitized solar cell module after long-term stability test under outdoor working condition. *Sol. Energy Mater. Sol. Cells* **93**, 893–897. (doi:10.1016/j.solmat.2008.10.022)
12. Huang X, Wang J, Yu D, Ye S, Zhang Q, Sun X. 2011 Spectral conversion for solar cell efficiency enhancement using YVO_4: Bi^{3+}, Ln^{3+} (Ln = Dy, Er, Ho, Eu, Sm, and Yb) phosphors. *J. Appl. Phys.* **109**, 113526. (doi:10.1063/1.3592889)
13. Llanos J, Castillo R, Espinoza D, Olivares R, Brito I. 2011 Red-emitting $Ln_{2-x}Eu_xTeO_6$: RE (Ln = La, Y; RE = Sm^{3+}, Gd^{3+}) phosphors prepared by the Pechini sol–gel method. *J. Alloys Compd.* **509**, 5295–5299. (doi:10.1016/j.jallcom.2011.01.161)
14. Llanos J, Castillo R, Martín I, Martín L, Haro-González P, González-Platas J. 2014 Energy transfer processes in Eu^{3+} doped nanocrystalline La_2TeO_6 phosphor. *J. Lumin.* **145**, 553–556. (doi:10.1016/j.jlumin.2013.08.005)
15. Alemany P, Moreira IDR, Castillo R, Llanos J. 2012 Electronic, structural, and optical properties of host materials for inorganic phosphors. *J. Alloys Compd.* **513**, 630–640. (10.1016/j.jallcom.2011.11.036)
16. Vega M, Fuentes S, Martín IR, Llanos J. 2017 Up-conversion photoluminescence of $BaTiO_3$ doped with Er^{3+} under excitation at 1500 nm. *Mater. Res. Bull.* **86**, 95–100. (doi:0.1016/j.materresbull.2016.10.001)
17. Qin C, Huang Y, Chen G, Shi L, Qiao X, Gan J, Seo HJ. 2009 Luminescence properties of a red phosphor europium tungsten oxide Eu_2WO_6. *Mater. Lett.* **63**, 1162–1164. (doi:10.1016/j.matlet.2009.02.018)
18. Llanos J, Olivares D, Manríquez V, Espinoza D, Brito I. 2015 Synthesis and luminescent properties of two different Y_2WO_6:Eu_{3+} phosphor phases. *J. Alloys Compd.* **628**, 352–356. (doi:10.1016/j.jallcom.2014.12.161)
19. Inorganic Crystal Structure Database, ICSD, Fachinformationzentrum Karlsruhe, Release 1/2016 (Coll. Code. #20955)
20. Zhang J, Shen H, Guo W, Wang S, Zhu C, Xue F, Hou J, Su H, Yuan Z. 2013 An upconversion $NaYF_4$:Yb^{3+}, Er^{3+}/TiO_2 core–shell nanoparticle photoelectrode for improved efficiencies of dye-sensitized solar cells. *J. Power Sources* **226**, 47–53. (doi:10.1016/j.jpowsour.2012.10.073)
21. Hafez H, Saif M, Abdel-Mottaleb M. 2011 Down-converting lanthanide doped TiO_2 photoelectrodes for efficiency enhancement of dye-sensitized solar cells. *J. Power Sources* **196**, 5792–5796. (doi:10.1016/j.jpowsour.2011.02.031)
22. Kumar V, Swami SK, Kumar A, Ntwaeaborwa O, Dutta V, Swart H. 2016 Eu^{3+} doped down shifting TiO_2 layer for efficient dye-sensitized solar cells. *J. Colloid Interface Sci.* **484**, 24–32. (doi:10.1016/j.jcis.2016.08.060)
23. Patterson A. 1939 The Scherrer formula for X-ray particle size determination. *Phys. Rev.* **56**, 978. (doi:10.1103/PhysRev.56.978)
24. Zhang Y, Yang Y, Jin S, Tian S, Li G, Jia J, Liao C, Yan C. 2001 Sol–Gel fabrication and electrical property of Nanocrystalline $(RE_2O_3)_{0.08}(ZrO_2)_{0.92}$ (RE = Sc, Y) thin films. *Chem. Mater.* **13**, 372–378. (doi:10.1021/cm0005236)
25. Xue XX, Ji W, Mao Z, Mao HJ, Wang Y, Wang X, Ruan WD, Zhao B, Lombardi JR. 2012 Raman investigation of nanosized TiO_2: effect of crystallite size and quantum confinement. *J. Phys. Chem. C* **116**, 8792–8797. (doi:10.1021/jp2122196)
26. Wang Z, Kawauchi H, Kashima T, Arakawa H. 2004 Significant influence of TiO_2 photoelectrode morphology on the energy conversion efficiency of N-719 due-sensitized solar cell. *Coord. Chem. Rev.* **248**, 1381–1389. (doi:10.1016/j.ccr.2004.03.006)
27. Koo H-J, Park J, Yoo B, Yoo K, Kim K, Park N-G. 2008 Size-dependent scattering efficiency in dye-sensitized solar cell. *Inorg. Chim. Acta* **361**, 677–683. (doi:10.1016/j.ica.2007.05.017)
28. Shen J, Li Z., Cheng R, Luo Q, Luo YD, Chen YW, Chen XH, Sun Z, Huang SM. 2014 Eu^{3+}-doped $NaGdF_4$ nanocrystal down-converting layer for efficient dye-sensitized solar cells. *ACS Appl. Mater. Interfaces* **6**, 17 454–17 462. (doi:10.1021/am505086e)
29. Hafez H, Wu J, Lan Z, Li Q, Xie G, Lin J, Huang M, Huang Y, Abdel-Mottaleb M. 2010 Enhancing the photoelectrical performance of dye-sensitized solar cells using TiO_2: Eu^{3+} nanorods. *Nanotechnology* **21**, 415201. (doi:10.1088/0957-4484/21/41/415201)
30. Huang J-H, Hung PY, Hu S-F, Liu R-S. 2010 Improvements efficiency of a dye-sensitized solar cell using Eu^{3+} modified TiO_2 nanoparticles as a secondary layer electrode. *J. Mater. Chem.* **20**, 6505–6511. (doi:10.1039/c0jm00549e)
31. Kim KS, Song H, Nam SH, Kim SM, Jeong H, Kim WB, Jung GY. 2012 Fabrication of an efficient light-scattering functionalized photoanode using periodically aligned ZnO hemisphere crystals for dye-sensitized solar cells. *Adv. Mater.* **24**, 792–798. (doi:10.1002/adma.201103985)
32. Park JH, Kim JY, Kim JH, Choi CJ, Kim H, Sung YE, Ahn K-S. 2011 Enhanced efficiency of dye-sensitized solar cells through $TiCl_4$-treated, nanoporous-layer-covered TiO_2 nanotube arrays. *J. Power Sources.* **196**, 8904–8908. (doi:10.1016/j.jpowsour.2011.06.063)
33. Yin X, Guo Y, Xue Z, Xu P, He M, Liu B. 2015 Performance enhancement of perovskite-sensitized mesoscopic solar cell using Nb-doped TiO_2 compact layer. *Nano Res.* **8**, 1997–2003. (doi:10.1007/s12274-015-0711-4)
34. Yin X, Xu Z, Guo Y, Xu P, He M. 2016 Ternary oxides in the TiO_2-ZnO system as efficient electron transport layers for perovskite solar cell with efficiency over 15%. *ACS Appl. Mater. Interfaces* **8**, 29 580–29 587. (doi:10.1021/acsami.6b09326)
35. Dong F, Guo Y, Xu P, Yin X, Li Y, He M. 2017 Hydrothermal growth of MoS_2/Co_3S_4 composites as efficient Pt-free counter electrodes for dye sensitized solar cells. *Sci. China Matter.* **60**, 295–303. (doi:10.1007/s40843-017-9009-8)
36. Llanos J, Brito I, Espinoza D, Seker R, Manidurai P. 2018 Data from: A down-shifting Eu^{3+}-doped Y_2WO_6/TiO_2 photoelectrode for improved light harvesting in dye-sensitized solar cells. Dryad Digital Repository. (http://dx.doi.org/10.5061/dryad.t04k1)